Joint Optimization of Stream Allocation and Beamforming and Combining Weights for the MIMO Interference Channel

Luis Miguel Cortés-Peña, John R. Barry, and Douglas M. Blough
School of Electrical and Computer Engineering
Georgia Institute of Technology
Atlanta, Georgia 30332–0250
{cortes, barry, doug.blough}@ece.gatech.edu

***Abstract*—We propose an algorithm to allocate streams and find the corresponding beamforming and combining weights that maximize the sum rate of a set of interfering multiple-input multiple-output (MIMO) links. Our algorithm iteratively computes the beamforming and combining weights of each link and determines how many streams, if any, are allocated to each link. Assigning zero streams to a link is desirable whenever the interference introduced by activating that link outweighs the throughput contributed by the link. We present numerical results to illustrate that our algorithm achieves a sum rate higher than previously reported algorithms at high interference, and that it achieves similar performance to the top-performing algorithms at medium and low interference. In one high-interference example with many links, our algorithm achieves a 65% higher sum rate than the best-known alternative.**

***Index Terms*—joint transceiver, minimum weighted sum mean-squared-error, sum rate**

I. Introduction

The performance of a wireless link can be improved without the need of additional spectrum or power by equipping the transmitter and the receiver with multiple antennas [1], leading to a multiple-input multiple-output (MIMO) link. A single MIMO link, in the absence of interference, can perform spatial multiplexing to transmit multiple streams in parallel. In the MIMO interference channel, where multiple interfering MIMO links are active simultaneously, MIMO links can perform a combination of spatial multiplexing and interference suppression, so that each transmitter can send multiple streams that can be decoded reliably and independently by their intended receivers. Computing the beamforming and combining weights that maximize the aggregate performance in the MIMO interference channel is, however, complicated by their inherent interdependence.

We tackle the problem of maximizing the sum rate of the MIMO interference channel. This problem includes the problems of determining which subset of transmitters should transmit, how many streams each transmitter should send (if any), and the corresponding beamforming and combining weights for each stream.

Most prior work has focused on a subset of these problems. The works of [2–4] focused only on computing the beamforming and combining weights. The works of [5–7] focused on determining how many streams each transmitter should transmit and their corresponding beamforming and combining weights (or transmit covariance matrices). However, the works of [5–7] require a separate algorithm to determine which transmitters should transmit. The works of [8–14] focused on determining which transmitters should transmit and how many streams each transmitter should transmit, but their solutions do not necessarily maximize the sum rate since the decisions are not based on the beamforming and combining weights of the links, which ultimately determine the performance. To the best of our knowledge, the only algorithms that consider all three problems are the MMSE algorithm from [15] and the SDP algorithm from [16].

In this paper, we present an algorithm that maximizes the sum rate for a set of interfering MIMO links by jointly optimizing which subset of transmitters should transmit, the number of streams for each transmitter (if any), and the beamforming and combining weights that support those streams. As a stepping stone, we first extend the results of Sampath et al. [17] to design, for a particular link, the joint optimal beamforming and combining weights that minimize the weighted sum MSE across all streams in the network. The transceiver has the ability to deactivate itself if it minimizes the weighted sum MSE. We show that the optimal combiner is a minimum mean-squared-error (MMSE) combiner, and that the optimal beamformer can be viewed as the MMSE combiner of a virtual network. Using our transceiver and the results from [5, 17, 18] that relate the minimum weighted sum MSE to the maximum weighted sum rate, we design our proposed algorithm to maximize the sum rate. Our algorithm finds which subset of transmitters should transmit since it will deactivate links, by allocating zero streams to them, if it improves the overall performance. Numerical results at high interference show that our algorithm outperforms previously

This research was supported in part by Grant CNS-1017248 from the National Science Foundation.

reported algorithms.

This paper is organized as follows. In Section II, we define our model for the physical layer. In Section III, we design the joint beamforming and combining weights for a single link. In Section IV, we review the relationship between the sum rate and the minimum weighted sum MSE. In Section V, we propose our algorithm for computing the beamforming and combining weights for all links. In Section VI, we present numerical results. Finally, in Section VII, we present our conclusions.

II. Physical-Layer Model

Consider a set of M half-duplex links. Let d_k be the number of multiplexed streams on link k, and let n_{t_k} and n_{r_k} be the number of antenna elements at the transmitter and receiver of link k, respectively. Let $\boldsymbol{H}_{kl} \in \mathbb{C}^{n_{r_k} \times n_{t_l}}$ be the matrix of complex channel gains between the antennas of transmitter l and those of receiver k.

The received vector at receiver k is given by

$$\boldsymbol{y}_k = \boldsymbol{H}_{kk}\boldsymbol{V}_k\boldsymbol{x}_k + \underbrace{\sum_{l=1,l\neq k}^{M} \boldsymbol{H}_{kl}\boldsymbol{V}_l\boldsymbol{x}_l + \boldsymbol{n}_k}_{\boldsymbol{z}_k}, \tag{1}$$

where $\boldsymbol{V}_k \in \mathbb{C}^{n_{t_k} \times d_k}$ is the beamforming matrix of transmitter k; $\boldsymbol{x}_k \in \mathbb{C}^{d_k}$ is the transmit signal vector from transmitter k, assumed to be independently encoded Gaussian codebook symbols with unit-energy so that $\mathbb{E}[\boldsymbol{x}_k\boldsymbol{x}_k^\dagger] = \boldsymbol{I}$, where $(\cdot)^\dagger$ is the conjugate transpose of $(\cdot)$; $\boldsymbol{n}_k \in \mathbb{C}^{n_{r_k}}$ is a vector of Gaussian noise elements with covariance matrix $\mathbb{E}[\boldsymbol{n}_k\boldsymbol{n}_k^\dagger] = \boldsymbol{R}_{\boldsymbol{n}_k}$; and $\boldsymbol{z}_k \in \mathbb{C}^{n_{r_k}}$ is the total received interference plus noise with covariance matrix

$$\boldsymbol{R}_{\bar{k}} = \mathbb{E}[\boldsymbol{z}_k\boldsymbol{z}_k^\dagger] = \sum_{l=1,l\neq k}^{M} \boldsymbol{H}_{kl}\boldsymbol{V}_l\boldsymbol{V}_l^\dagger\boldsymbol{H}_{kl}^\dagger + \boldsymbol{R}_{\boldsymbol{n}_k}. \tag{2}$$

In order to meet a power constraint of p_k, the beamforming weights for transmitter k must satisfy $\operatorname{tr}\left(\boldsymbol{V}_k\boldsymbol{V}_k^\dagger\right) \leq p_k$. The instantaneous capacity in bits/sec/Hz of link k before combining is given by [19]

$$C_k = \log_2\left|\boldsymbol{I} + \boldsymbol{R}_{\bar{k}}^{-1}\boldsymbol{H}_{kk}\boldsymbol{V}_k\boldsymbol{V}_k^\dagger\boldsymbol{H}_{kk}^\dagger\right|. \tag{3}$$

After combining, the received signal at receiver k is given by

$$\hat{\boldsymbol{x}}_k = \boldsymbol{U}_k^\dagger\boldsymbol{y}_k, \tag{4}$$

where $\boldsymbol{U}_k \in \mathbb{C}^{n_{r_k} \times d_k}$ is the combining matrix of receiver k, and the instantaneous capacity in bits/sec/Hz is given by

$$\hat{C}_k = \log_2\left|\boldsymbol{I} + \left(\boldsymbol{U}_k^\dagger\boldsymbol{R}_{\bar{k}}\boldsymbol{U}_k\right)^{-1}\boldsymbol{U}_k^\dagger\boldsymbol{H}_{kk}\boldsymbol{V}_k\boldsymbol{V}_k^\dagger\boldsymbol{H}_{kk}^\dagger\boldsymbol{U}_k\right|. \tag{5}$$

III. Jointly Computing the Beamforming and Combining Weights for a Single Link

We begin by optimizing the beamforming and combining weights for a single link in the presence of interfering links as a stepping stone towards computing the beamforming and combining weights for all links. In this section, we design the joint transceiver that minimizes the weighted sum MSE across all streams in the network. We choose the weighted sum MSE criterion because, as we will review in Section IV, it reduces to maximizing the sum rate as a special case [5, 17, 18]. Later, in Section V, we will use the joint transceiver to design an algorithm that computes the beamforming and combining weights of all links.

A. The Minimum Weighted Sum MSE Problem

We formulate the weighted sum MSE optimization for the beamforming and combining weights of link k as

$$(\boldsymbol{V}_k^*, \boldsymbol{U}_k^*) = \arg\min_{\boldsymbol{V}_k,\boldsymbol{U}_k} \sum_{l=1}^{M} \operatorname{tr}(\boldsymbol{W}_l\boldsymbol{E}_l)$$
$$\text{such that } \operatorname{tr}\left(\boldsymbol{V}_k\boldsymbol{V}_k^\dagger\right) \leq p_k, \tag{6}$$

where

$$\boldsymbol{E}_k = \mathbb{E}[(\hat{\boldsymbol{x}}_k - \boldsymbol{x}_k)(\hat{\boldsymbol{x}}_k - \boldsymbol{x}_k)^\dagger] \tag{7}$$

is the error covariance matrix of link k and contains the MSE of the streams of link k in the diagonal. In (6), $\boldsymbol{W}_k \in \mathbb{R}^{d_k \times d_k}$ is a diagonal matrix of nonnegative weights associated with the MSE of the streams of link k.

Note that due to the inequality constraint $\operatorname{tr}\left(\boldsymbol{V}_k\boldsymbol{V}_k^\dagger\right) \leq p_k$ in (6), we have formulated the problem so that the link will deactivate itself by setting $\boldsymbol{V}_k$ to zero if it is optimal to do so. As we will see using numerical results in Section VI, deactivating links is desirable at high interference since interference caused by one link highly affects the performance of all other links in the network.

B. The Minimum Weighted Sum MSE Solution

The solution to (6) can be expressed in terms of the following compact singular-value decomposition (SVD):

$$\boldsymbol{R}_{\bar{k}}^{-1/2}\boldsymbol{H}_{kk}\boldsymbol{P}_{\bar{k}}^{-1/2} = \boldsymbol{F}_k\boldsymbol{D}_k\boldsymbol{G}_k^\dagger, \tag{8}$$

where $\boldsymbol{D}_k \in \mathbb{R}^{d_k \times d_k}$ is a diagonal matrix containing the nonzero singular values of $\boldsymbol{R}_{\bar{k}}^{-1/2}\boldsymbol{H}_{kk}\boldsymbol{P}_{\bar{k}}^{-1/2}$ ordered in decreasing order from top left to bottom right; $\boldsymbol{F}_k \in \mathbb{C}^{n_{r_k} \times d_k}$ and $\boldsymbol{G}_k \in \mathbb{C}^{n_{t_k} \times d_k}$ have orthonormal column vectors that correspond to the left and right eigenvectors of $\boldsymbol{R}_{\bar{k}}^{-1/2}\boldsymbol{H}_{kk}\boldsymbol{P}_{\bar{k}}^{-1/2}$ with nonzero singular values, respectively; and $\boldsymbol{P}_{\bar{k}}$ is

$$\boldsymbol{P}_{\bar{k}} = \sum_{l=1,l\neq k}^{M} \boldsymbol{H}_{lk}^\dagger\boldsymbol{U}_l\boldsymbol{W}_l\boldsymbol{U}_l^\dagger\boldsymbol{H}_{lk} + \mu_k\boldsymbol{I}, \tag{9}$$

where $\mu_k \geq 0$ is a Lagrange multiplier that must satisfy the Karush-Kuhn-Tucker (KKT) conditions for the optimization of (6) (see Appendix). The SVD in (8) requires that $\boldsymbol{P}_{\bar{k}}$ be invertible, which is clearly true whenever $\mu_k > 0$, and which we conjecture to be true whenever $\mu_k = 0$.

In the following, we will assume that we already know μ_k and present the beamforming and combining weights that solve (6). Later in this section, we will show how to obtain μ_k.

Theorem 1. *The joint beamforming and combining weights that solve* (6) *are given by*

$$\boldsymbol{V}_k = \boldsymbol{P}_{\bar{k}}^{-1/2}\boldsymbol{G}_k\boldsymbol{\Theta}_k, \tag{10}$$

$$\boldsymbol{U}_k = \boldsymbol{R}_{\bar{k}}^{-1/2}\boldsymbol{F}_k\boldsymbol{\Phi}_k, \tag{11}$$

where

$$\boldsymbol{\Theta}_k = \left(\boldsymbol{W}_k^{1/2}\boldsymbol{D}_k^{-1} - \boldsymbol{D}_k^{-2}\right)_+^{1/2}, \tag{12}$$

$$\boldsymbol{\Phi}_k = \boldsymbol{W}_k^{-1/2}\boldsymbol{\Theta}_k, \tag{13}$$

and $(\cdot)_+$ *is the matrix* $(\cdot)$ *with the negative entries replaced with zeros.*

Proof: See Appendix. □

Using Theorem 1, we can rewrite (4) as

$$\hat{\boldsymbol{x}}_k = \boldsymbol{\Phi}_k\left(\boldsymbol{D}_k\boldsymbol{\Theta}_k\boldsymbol{x}_k + \hat{\boldsymbol{n}}_k\right), \tag{14}$$

where $\hat{\boldsymbol{n}}_k = \boldsymbol{F}_k^\dagger\boldsymbol{R}_{\bar{k}}^{-1/2}\boldsymbol{z}_k$ is a vector of white Gaussian noise satisfying

$$\mathbb{E}[\hat{\boldsymbol{n}}_k\hat{\boldsymbol{n}}_k^\dagger] = \boldsymbol{F}_k^\dagger\boldsymbol{R}_{\bar{k}}^{-1/2}\boldsymbol{R}_{\bar{k}}\boldsymbol{R}_{\bar{k}}^{-1/2}\boldsymbol{F}_k = \boldsymbol{I}.$$

Therefore, the beamforming and combining weights in (10) and (11) diagonalize the MIMO channel.

To complete the solution to (6), we must find μ_k. Because a closed-form solution to μ_k is unknown, and because $\mathrm{tr}(\boldsymbol{V}_k\boldsymbol{V}_k^\dagger)$ is a decreasing function of μ_k [15], we search for the value of μ_k as follows. First, we test for $\mu_k = 0$. If the beamforming weights satisfy $\mathrm{tr}(\boldsymbol{V}_k\boldsymbol{V}_k^\dagger) \leq p_k$, then the search is done because all KKT conditions are satisfied. If, however, $\boldsymbol{P}_{\bar{k}}$ is singular or $\mathrm{tr}(\boldsymbol{V}_k\boldsymbol{V}_k^\dagger) > p_k$, then we search for the $\mu_k > 0$ such that $\mathrm{tr}(\boldsymbol{V}_k\boldsymbol{V}_k^\dagger) = p_k$, thereby satisfying all KKT conditions. In our simulations, we use the bisection method to perform the search for $\mu_k > 0$.

C. Interpreting the Solution

The beamforming and combining weights in (10) and (11) have three components that can be inter-related through the use of a virtual network in which receivers become virtual transmitters and transmitters become virtual receivers. The concept of a virtual network has been previously used to aid the design of the transmitter's beamforming weights in the works of [2–4, 20].

To build the virtual network that relates (10) and (11), let us define $\overleftarrow{\boldsymbol{H}}_{lk} = \boldsymbol{H}_{kl}^\dagger$ as the virtual MIMO channel between the virtual transmitter of link k and the virtual receiver of link l; $\overleftarrow{\boldsymbol{V}}_k = \boldsymbol{U}_k\boldsymbol{W}_k^{1/2}$ as the virtual beamforming weights of link k; $\overleftarrow{\boldsymbol{U}}_k = \boldsymbol{V}_k\boldsymbol{W}_k^{-1/2}$ as the virtual combining weights of link k; and $\overleftarrow{\boldsymbol{R}}_{n_k} = \mu_k\boldsymbol{I}$ as the virtual noise covariance of the virtual receiver of link k.

Figure 1 shows a block diagram of the transmit and receive structure for link k and highlights the three components of the joint transceiver using dotted boxes. The three components and their functions are as follows:

- *Whitening Component* – The first component of the transceiver is a whitening component. At the receiver side, the receiver whitens the interference plus noise of the received signal. In Figure 1, the dashed box at the receiver groups the receiver-side whitener and the components that are whitened. At the transmitter side, this whitening component performs a similar function by whitening a "virtual" interference plus noise with covariance matrix given by

$$\overleftarrow{\boldsymbol{R}}_{\bar{k}} = \sum_{l=1,l\neq k}^{M}\overleftarrow{\boldsymbol{H}}_{kl}\overleftarrow{\boldsymbol{V}}_l\overleftarrow{\boldsymbol{V}}_l^\dagger\overleftarrow{\boldsymbol{H}}_{kl}^\dagger + \overleftarrow{\boldsymbol{R}}_{\boldsymbol{n}_k} = \boldsymbol{P}_{\bar{k}}. \tag{15}$$

  In Figure 1, the dashed box at the transmitter groups the transmitter-side whitener and the components of the real network that are whitened.
- *Rotating Component* – The second component is a rotating component. Using this component, both the transmitter and the receiver rotate their signal so as to diagonalize their MIMO channel. The rotating matrices are chosen based on the SVD of the cascade of the whitening components and the MIMO channel ($\boldsymbol{R}_{\bar{k}}^{-1/2}\boldsymbol{H}_{kk}\boldsymbol{P}_{\bar{k}}^{-1/2}$).
- *Power Allocating Component* – The third component is a power allocating component that scales each element of the signal vector. Due to the $(\cdot)_+$ operator in (12), the power allocating component at the transmitter can potentially prevent some, if not all, streams from being transmitted. On the virtual network, the receiver's power allocating component acts similarly to the transmitter's power allocating component by scaling some signal elements and even reducing the number of streams on the virtual link.

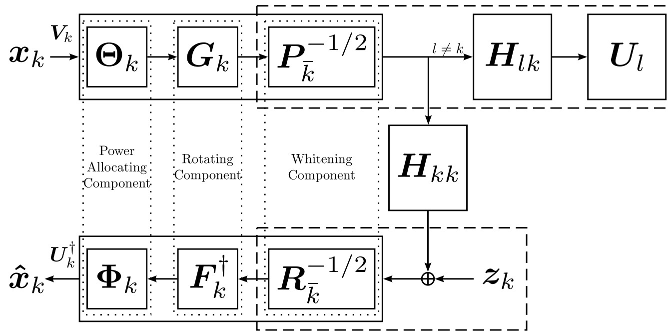

Fig. 1. Block diagram of the components of the joint beamforming and combining weights.

Using the MMSE combining weights for link k, as given by [5, 15]

$$\boldsymbol{U}_k^{\mathrm{MMSE}} = \left(\boldsymbol{H}_{kk}\boldsymbol{V}_k\boldsymbol{V}_k^\dagger\boldsymbol{H}_{kk}^\dagger + \boldsymbol{R}_{\bar{k}}\right)^{-1}\boldsymbol{H}_{kk}\boldsymbol{V}_k, \tag{16}$$

we can further relate the joint beamforming and combining weights. Specifically, it is easy to show that if the beamforming weights are given by (10), then the MMSE combining weights will be equal to (11). Similarly, at the transmitter side, it is easy to show that if the combining weights are given by (11), then the MMSE combining weights of the virtual network are given by $\overleftarrow{U}_k^{\text{MMSE}} = P_{\bar{k}}^{-1/2} G_k \Phi_k$, and so the beamforming weights of the real network are given by (10).

IV. The Weighted Sum MSE and the Sum Rate

We have chosen the weighted sum MSE as our objective function because with a proper choice of the error weight matrix $\boldsymbol{W}_k$, minimizing the weighted sum MSE also maximizes the sum rate. This relationship was exploited for the single MIMO link in the absence of interference by Sampath et al. in [17], for the MIMO broadcast channel by Christensen et al. in [18], and for the MIMO interference channel by Negro et al. in [5]. In the latter, the authors find that the gradient of the sum rate and the gradient of the weighted sum MSE are equal if

$$\boldsymbol{W}_k = \boldsymbol{I} + \boldsymbol{B}_k^\dagger \boldsymbol{V}_k^\dagger \boldsymbol{H}_{kk}^\dagger \boldsymbol{R}_{\bar{k}}^{-1} \boldsymbol{H}_{kk} \boldsymbol{V}_k \boldsymbol{B}_k, \tag{17}$$

where $\boldsymbol{B}_k$ is an arbitrary unitary matrix.

Notice that $\boldsymbol{W}_k$ in (17) is a function of $\boldsymbol{V}_k$, which is itself one of the variables to optimize. To solve this interdependency, the authors of [5] propose to compute $\boldsymbol{W}_k$ and $\boldsymbol{V}_k$ in separate steps in an iterative algorithm. We follow the same approach.

In our formulation of (6), we require that $\boldsymbol{W}_k$ be diagonal. To guarantee that (17) is always diagonal, we choose $\boldsymbol{B}_k$ in (17) from the following SVD:

$$\boldsymbol{A}_k \boldsymbol{S}_k \boldsymbol{B}_k^\dagger = \boldsymbol{R}_{\bar{k}}^{-1/2} \boldsymbol{H}_k \boldsymbol{V}_k, \tag{18}$$

where $\boldsymbol{S}_k \in \mathbb{R}^{d_k \times d_k}$ is a diagonal matrix containing the singular values of $\boldsymbol{R}_{\bar{k}}^{-1/2} \boldsymbol{H}_k \boldsymbol{V}_k$ ordered in decreasing order from top left to bottom right; $\boldsymbol{B}_k \in \mathbb{C}^{d_k \times d_k}$ is a unitary matrix; and $\boldsymbol{A}_k \in \mathbb{C}^{n_{r_k} \times d_k}$ has orthonormal column vectors. This way, (17) becomes

$$\boldsymbol{W}_k = \boldsymbol{I} + \boldsymbol{S}_k^2. \tag{19}$$

This choice of $\boldsymbol{B}_k$ was used by Christensen et al. in [18] to design the WSRBF-WMMSE-D algorithm with diagonal weighting matrix for the MIMO broadcast channel.

V. Computing the Beamforming and Combining Weights for all Links

We now propose an algorithm for maximizing the sum rate of a set of interfering MIMO links by jointly optimizing the number of streams (if any) on each link as well as their beamforming and combining weights.

The proposed algorithm is summarized in Figure 2. Our algorithm begins by activating all links and allocating the maximum number of streams at every transmitter, as shown on Line 1 of Figure 2, where $\boldsymbol{I}_{n_{t_k} \times d_k}$ is an $n_{t_k} \times d_k$ matrix with ones on its diagonal and zeros elsewhere. Then, on lines 2-6, the algorithm computes the beamforming and combining weights iteratively. In Line 3, the receivers compute their interference-plus-noise covariance, error weights and combining weights using the previously computed beamforming weights. In Line 4, the transmitters compute their beamforming weights using the previously computed interference-plus-noise covariance, error weights, and combining weights. During the computation of the beamforming weights, a transmitter will disable, or re-enable, itself if it determines that doing so improves the overall performance.

Using the technique from [18], we can show that this algorithm is guaranteed to converge, since at every iteration the algorithm moves monotonically towards a bounded objective.

1: Initialize $d_k = \text{rank}(\boldsymbol{H}_{kk})$, $\boldsymbol{V}_k = \sqrt{\frac{1}{d_k}} \boldsymbol{I}_{n_{t_k} \times d_k}$ for all $k \in \{1, \ldots, M\}$;
2: **for** $iteration \leftarrow 1$ **to** N_{max} **do**
3: Compute $\boldsymbol{R}_{\bar{k}}$ using (2), $\boldsymbol{W}_k$ using (19), and $\boldsymbol{U}_k^{\text{MMSE}}$ using (16) for all $k \in \{1, \ldots, M\}$;
4: Compute $\boldsymbol{V}_k$ using (10) for all $k \in \{1, \ldots, M\}$;
5: Stop if the maximum absolute value of the difference of elements between the previous $\boldsymbol{Q}_k = \boldsymbol{V}_k \boldsymbol{V}_k^\dagger$ and the newly computed $\boldsymbol{Q}_k$ is less than ϵ for all $k \in \{1, \ldots, M\}$;
6: **end for**

Fig. 2. Pseudocode of proposed algorithm for computing the beamforming and combining weights of all links.

VI. Numerical Results

In this section we present numerical results comparing the proposed algorithm to previously reported algorithms in various levels of interference. For all simulations, we fix the distance between the transmitter and its corresponding receiver to 50 meters. We set each node to have four antenna elements. Also, we assume that noise at each receiver is white, satisfying $\boldsymbol{R}_{\boldsymbol{n}_k} = \boldsymbol{I}$ for all $k \in \{1, \ldots, M\}$. We assume a "quasi-static" flat-fading Rayleigh model where the channel is assumed constant for the duration of a burst, but random between bursts [21]. We set the reference signal-to-noise ratio and interference-to-noise ratio at one meter to 65.3 dB. We assume a path-loss exponent of three. We uniformly distribute the center of each link within a circle of a given radius. Also, we uniformly distribute the angles from the horizontal axis to the line that goes through the transmitter and receiver of every link from zero to 2π. For all algorithms, we initialize the beamforming weights as shown on Line 1 of Figure 2, and use the convergence criterion as shown on Line 5 of Figure 2 with $\epsilon = 0.0001$. Additionally, we set the maximum number of iterations to $N_{max} = 10000$. If an algorithm reaches the maximum number of iterations, the algorithm stops and we record the sum rate.

In the following, we consider two scenarios. In Section VI-A, we fix the number of links and vary the radius of the circle in which the links are placed. In Section VI-B, we fix the radius of the circle and vary the number of links.

A. Sum Rate Versus Circle Radius

We consider ten MIMO links and vary the radius of the circle in which these links are placed. Figure 3 shows the sum rate, averaged over 100 trials, plotted as a function of the radius of the circle in which the center of the links are placed. A large radius in Figure 3 corresponds to a sparse

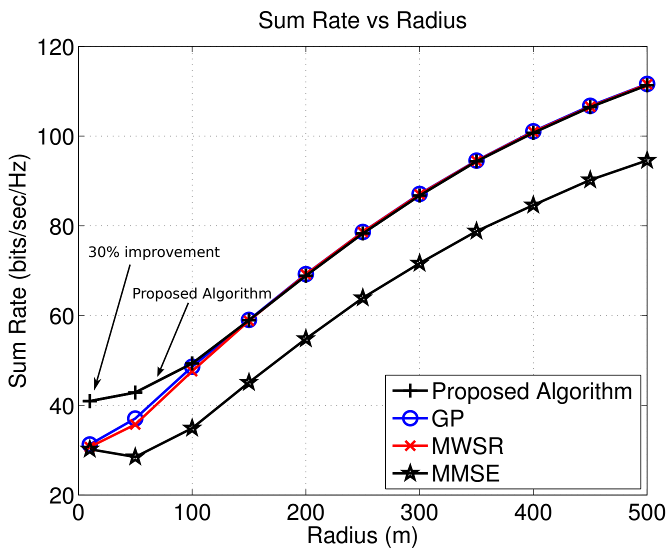

Fig. 3. Sum rate as a function of the radius of the circle where the center of the ten links are placed.

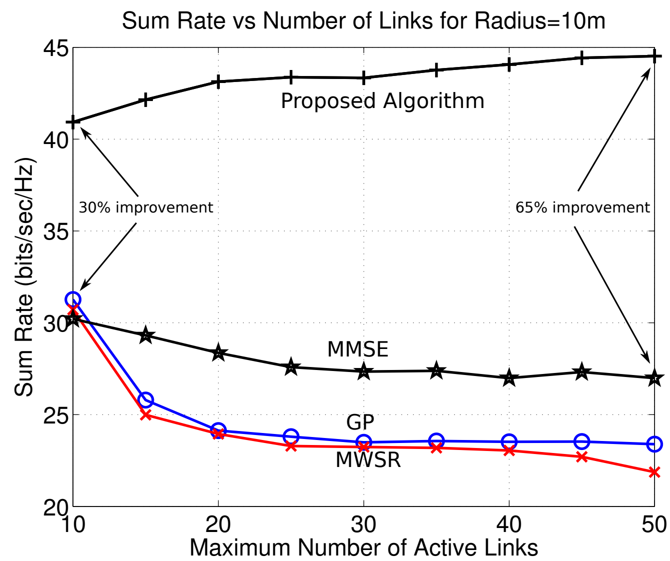

Fig. 4. Sum rate as a function of the maximum number of active links when the radius of the circle is fixed to ten meters.

scenario where interference from other links is low. In contrast, a small radius in Figure 3 corresponds to a dense scenario where interference from other links is high. In Figure 3, we show results for the two top-performing previously reported algorithms, namely, the MWSR algorithm from [5] and the GP algorithm from [6]. We also show results for the MMSE algorithm from [15], since, as we will see in Section VI-B, it has good performance when the number of links is high. We do not include a comparison against the SDP algorithm from [16], because on the few sample runs we attempted, we found the execution time of the SDP algorithm to be about two to three orders of magnitude higher than other methods.

The results of Figure 3 show that our proposed algorithm achieves at least 30% higher sum rate at the lowest radius tested (10 meters), as compared to the other algorithms. In this range, interference is high and the degrees-of-freedom available from the multiple antennas on the nodes are not enough to support high performance on all links. Our proposed algorithm overcomes this limitation by deactivating some links so that the remaining links achieve higher aggregate performance. The MMSE algorithm from [15] also has the capability to deactivate links, but because the algorithm minimizes the unweighted sum MSE, it does not necessarily achieve a high sum rate. Figure 3 also shows that our proposed algorithm achieves similar sum rate to those of the previously reported algorithms at medium and low interference.

In terms of CPU time and number of iterations for this simulation, the MMSE algorithm requires the least, followed by the MWSR, then our proposed algorithm, then the GP.

B. Sum Rate Versus Number of Links at High Interference

In this section, we fix the radius of the circle to ten meters and vary the number of links placed within this circle. Figure 4 shows the sum rate, averaged over 100 trials, plotted as a function of the maximum number of active links when the radius of the circle is fixed to ten meters. The results show that as the number of links increases, the performance of the GP, MWSR, and MMSE algorithms decrease while the performance of the proposed algorithm increases. Our algorithm achieves a sum rate that is at least 65% better than the sum rate of the other algorithms at the largest number of links tested. The decrease in performance of the GP and the MWSR is due to the algorithms being unable to deactivate links. The MMSE algorithm also suffers performance loss but performs better than the GP and the MWSR because it is able to deactivate links. The proposed algorithm achieves high performance since it is able to deactivate links, and its performance increases as the number of links increases, since the algorithm has diversity on which links to activate and deactivate.

In terms of CPU time and number of iterations for this simulation, the MMSE algorithm requires the least, followed by our proposed algorithm, then the MWSR, and then the GP.

VII. Conclusions

We have presented an algorithm for maximizing the sum rate of a set of interfering MIMO links. Our algorithm jointly optimizes which link should be active, the number of streams (if any) on each link, and their corresponding beamforming and combining weights. Our simulation results showed that, in terms of sum rate, the proposed algorithm is able to outperform previously reported algorithms at high interference and maintain high performance at medium and low interference. Also, our simulation results showed that at high interference, the sum rate of our proposed algorithm increases as the number of links increases, because the proposed algorithm can deactivate links and has diversity on which links to deactivate.

APPENDIX
PROOF OF THEOREM 1

Proof: Before we begin, let us expand (8) to include the zero singular values as follows. Let

$$\boldsymbol{R}_{\bar{k}}^{-1/2}\boldsymbol{H}_{kk}\boldsymbol{P}_{\bar{k}}^{-1/2} = \begin{bmatrix}\boldsymbol{F}_k & \widetilde{\boldsymbol{F}}_k\end{bmatrix}\begin{bmatrix}\boldsymbol{D}_k & \boldsymbol{0}\\ \boldsymbol{0} & \boldsymbol{0}\end{bmatrix}\begin{bmatrix}\boldsymbol{G}_k & \widetilde{\boldsymbol{G}}_k\end{bmatrix}^{\dagger} \tag{20}$$

by singular-value decomposition (SVD), where $\widetilde{\boldsymbol{F}}_k \in \mathbb{C}^{n_{r_k}\times(n_{r_k}-d_k)}$ and $\widetilde{\boldsymbol{G}}_k \in \mathbb{C}^{n_{t_k}\times(n_{t_k}-d_k)}$ have orthonormal column vectors that correspond to the left and right eigenvectors of $\boldsymbol{R}_{\bar{k}}^{-1/2}\boldsymbol{H}_{kk}\boldsymbol{P}_{\bar{k}}^{-1/2}$ with zero singular values, respectively.

We will first prove that the joint beamforming and combining weights have the structure given in (10) and (11), where $\boldsymbol{\Phi}_k$ and $\boldsymbol{\Theta}_k$ are arbitrary $d_k \times d_k$ matrices. The Lagrangian for (6) is given by

$$\begin{aligned} L(\boldsymbol{V}_k, \boldsymbol{U}_k, \mu_k) = &\sum_{k=1}^{M} \operatorname{tr}(\boldsymbol{W}_k\boldsymbol{E}_k) \\ &+ \mu_k\left(\operatorname{tr}\left(\boldsymbol{V}_k\boldsymbol{V}_k^{\dagger}\right) - p_k\right). \end{aligned} \tag{21}$$

where μ_k is the Lagrange multiplier for link k, and

$$\begin{aligned} \boldsymbol{E}_k = &\boldsymbol{U}_k^{\dagger}\boldsymbol{H}_{kk}\boldsymbol{V}_k\boldsymbol{V}_k^{\dagger}\boldsymbol{H}_{kk}^{\dagger}\boldsymbol{U}_k + \boldsymbol{U}_k^{\dagger}\boldsymbol{R}_{\bar{k}}\boldsymbol{U}_k \\ &- \boldsymbol{U}_k^{\dagger}\boldsymbol{H}_{kk}\boldsymbol{V}_k - \boldsymbol{V}_k^{\dagger}\boldsymbol{H}_{kk}^{\dagger}\boldsymbol{U}_k + \boldsymbol{I}, \end{aligned} \tag{22}$$

by expanding (7) using (4). The Karush-Kuhn-Tucker (KKT) conditions to solve the optimization problem in (6) are

$$\nabla_{\boldsymbol{U}_k^{\dagger}} L = \boldsymbol{0}, \tag{23}$$

$$\nabla_{\boldsymbol{V}_k^{\dagger}} L = \boldsymbol{0}, \tag{24}$$

$$\operatorname{tr}\left(\boldsymbol{V}_k\boldsymbol{V}_k^{\dagger}\right) - p_k \le 0, \tag{25}$$

$$\mu_k\left(\operatorname{tr}\left(\boldsymbol{V}_k\boldsymbol{V}_k^{\dagger}\right) - p_k\right) = 0, \tag{26}$$

$$\mu_k \ge 0. \tag{27}$$

Setting the gradient of L with respect to $\boldsymbol{U}_k^{\dagger}$ to zero, we get

$$\boldsymbol{H}_{kk}\boldsymbol{V}_k = \boldsymbol{H}_{kk}\boldsymbol{V}_k\boldsymbol{V}_k^{\dagger}\boldsymbol{H}_{kk}\boldsymbol{U}_k + \boldsymbol{R}_{\bar{k}}\boldsymbol{U}_k, \tag{28}$$

and the gradient of L with respect to $\boldsymbol{V}_k^{\dagger}$ to zero, we get

$$\begin{aligned} \boldsymbol{H}_{kk}^{\dagger}\boldsymbol{U}_k\boldsymbol{W}_k = &\boldsymbol{H}_{kk}^{\dagger}\boldsymbol{U}_k\boldsymbol{W}_k\boldsymbol{U}_k^{\dagger}\boldsymbol{H}_{kk}\boldsymbol{V}_k \\ &+ \sum_{l=1,l\neq k}^{M} \boldsymbol{H}_{lk}^{\dagger}\boldsymbol{U}_l\boldsymbol{W}_l\boldsymbol{U}_l^{\dagger}\boldsymbol{H}_{lk}\boldsymbol{V}_k + \mu_k\boldsymbol{V}_k. \end{aligned} \tag{29}$$

Now, assume the most general expression for the beamforming and combining weights of link k as follows:

$$\boldsymbol{U}_k = \underbrace{\boldsymbol{R}_{\bar{k}}^{-1/2}\boldsymbol{F}_k\boldsymbol{\Phi}_k}_{\boldsymbol{U}_{||}} + \underbrace{\boldsymbol{R}_{\bar{k}}^{-1/2}\widetilde{\boldsymbol{F}}_k\widetilde{\boldsymbol{\Phi}}_k}_{\boldsymbol{U}_{\perp}}, \tag{30}$$

$$\boldsymbol{V}_k = \underbrace{\boldsymbol{P}_{\bar{k}}^{-1/2}\boldsymbol{G}_k\boldsymbol{\Theta}_k}_{\boldsymbol{V}_{||}} + \underbrace{\boldsymbol{P}_{\bar{k}}^{-1/2}\widetilde{\boldsymbol{G}}_k\widetilde{\boldsymbol{\Theta}}_k}_{\boldsymbol{V}_{\perp}}, \tag{31}$$

where $\widetilde{\boldsymbol{\Phi}}_k$ is any $(n_{r_k}-d_k)\times d_k$ matrix and $\widetilde{\boldsymbol{\Theta}}_k$ is any $(n_{t_k}-d_k)\times d_k$ matrix. Note that $\boldsymbol{R}_{\bar{k}}$ does not impose any constraint on (30) since $\boldsymbol{R}_{\bar{k}}$ is square and full rank. Also, $\boldsymbol{P}_{\bar{k}}$ does not impose any constraint on (31) since $\boldsymbol{P}_{\bar{k}}$ is square and assumed full rank.

To get (11) for arbitrary $\boldsymbol{\Phi}_k$, we premultiply (28) with $\boldsymbol{U}_{\perp}^{\dagger}$ to get

$$\boldsymbol{U}_{\perp}^{\dagger}\boldsymbol{R}_{\bar{k}}\boldsymbol{U}_k = \boldsymbol{0} \tag{32}$$

since

$$\begin{aligned} \boldsymbol{U}_{\perp}^{\dagger}\boldsymbol{H}_{kk}\boldsymbol{V}_k &= \widetilde{\boldsymbol{\Phi}}_k^{\dagger}\widetilde{\boldsymbol{F}}_k^{\dagger}\boldsymbol{R}_{\bar{k}}^{-1/2}\boldsymbol{H}_{kk}\boldsymbol{P}_{\bar{k}}^{-1/2}\left(\boldsymbol{G}_k\boldsymbol{\Theta}_k + \widetilde{\boldsymbol{G}}_k\widetilde{\boldsymbol{\Theta}}_k\right) \\ &= \widetilde{\boldsymbol{\Phi}}_k^{\dagger}\widetilde{\boldsymbol{F}}_k^{\dagger}\boldsymbol{F}_k\boldsymbol{D}_k\boldsymbol{G}_k^{\dagger}\left(\boldsymbol{G}_k\boldsymbol{\Theta}_k + \widetilde{\boldsymbol{G}}_k\widetilde{\boldsymbol{\Theta}}_k\right) = \boldsymbol{0}, \end{aligned}$$

and $\widetilde{\boldsymbol{F}}_k^{\dagger}\boldsymbol{F}_k = \boldsymbol{0}$. Expanding (32), we get

$$\begin{aligned} \widetilde{\boldsymbol{\Phi}}_k^{\dagger}\widetilde{\boldsymbol{F}}_k^{\dagger}\boldsymbol{F}_k\boldsymbol{\Phi}_k + \widetilde{\boldsymbol{\Phi}}_k^{\dagger}\widetilde{\boldsymbol{F}}_k^{\dagger}\widetilde{\boldsymbol{F}}_k\widetilde{\boldsymbol{\Phi}}_k &= \boldsymbol{0}, \\ \widetilde{\boldsymbol{\Phi}}_k^{\dagger}\widetilde{\boldsymbol{\Phi}}_k &= \boldsymbol{0}, \end{aligned} \tag{33}$$

since $\widetilde{\boldsymbol{F}}_k^{\dagger}\widetilde{\boldsymbol{F}}_k = \boldsymbol{I}$. From (33), it is clear that $\widetilde{\boldsymbol{\Phi}}_k = \boldsymbol{0}$, and therefore $\boldsymbol{U}_{\perp} = \boldsymbol{0}$.

To get (10) for arbitrary $\boldsymbol{\Theta}_k$, we premultiply (29) by $\boldsymbol{V}_{\perp}^{\dagger}$ to get

$$\begin{aligned} \boldsymbol{V}_{\perp}^{\dagger}\left(\sum_{l=1,l\neq k}^{M}\boldsymbol{H}_{lk}^{\dagger}\boldsymbol{U}_l\boldsymbol{W}_l\boldsymbol{U}_l^{\dagger}\boldsymbol{H}_{lk} + \mu_k\boldsymbol{I}\right)\boldsymbol{V}_k &= \boldsymbol{0}, \\ \boldsymbol{V}_{\perp}^{\dagger}\boldsymbol{P}_{\bar{k}}\boldsymbol{V}_k &= \boldsymbol{0}, \end{aligned} \tag{34}$$

because

$$\begin{aligned} \boldsymbol{V}_{\perp}^{\dagger}\boldsymbol{H}_{kk}^{\dagger}\boldsymbol{U}_k &= \widetilde{\boldsymbol{\Theta}}_k^{\dagger}\widetilde{\boldsymbol{G}}_k^{\dagger}\boldsymbol{P}_{\bar{k}}^{-1/2}\boldsymbol{H}_{kk}^{\dagger}\boldsymbol{R}_{\bar{k}}^{-1/2}\boldsymbol{F}_k\boldsymbol{\Phi}_k \\ &= \widetilde{\boldsymbol{\Theta}}_k^{\dagger}\widetilde{\boldsymbol{G}}_k^{\dagger}\boldsymbol{G}_k^{\dagger}\boldsymbol{D}_k\boldsymbol{F}_k^{\dagger}\boldsymbol{F}_k\boldsymbol{\Phi}_k = \boldsymbol{0}, \end{aligned}$$

and $\widetilde{\boldsymbol{G}}_k^{\dagger}\boldsymbol{G}_k^{\dagger} = \boldsymbol{0}$. Expanding (34), we get

$$\begin{aligned} \widetilde{\boldsymbol{\Theta}}_k^{\dagger}\widetilde{\boldsymbol{G}}_k^{\dagger}\boldsymbol{G}_k\boldsymbol{\Theta}_k + \widetilde{\boldsymbol{\Theta}}_k^{\dagger}\widetilde{\boldsymbol{G}}_k^{\dagger}\widetilde{\boldsymbol{G}}_k\widetilde{\boldsymbol{\Theta}}_k &= \boldsymbol{0}, \\ \widetilde{\boldsymbol{\Theta}}_k^{\dagger}\widetilde{\boldsymbol{\Theta}}_k &= \boldsymbol{0}, \end{aligned} \tag{35}$$

since $\widetilde{\boldsymbol{G}}_k^{\dagger}\widetilde{\boldsymbol{G}}_k = \boldsymbol{I}$. It is clear from (35) that $\widetilde{\boldsymbol{\Theta}}_k = \boldsymbol{0}$, and therefore $\boldsymbol{V}_{\perp} = \boldsymbol{0}$.

Now we will prove that matrices $\boldsymbol{\Phi}_k$ in (11) and $\boldsymbol{\Theta}_k$ in (10) are diagonal matrices. Premultiplying (28) with $\boldsymbol{U}_k^{\dagger}$, premultiplying (29) with $\boldsymbol{V}_k^{\dagger}$, and simplifying using (20) we get

$$\boldsymbol{\Phi}_k^{\dagger}\boldsymbol{D}_k\boldsymbol{\Theta}_k = \boldsymbol{\Phi}_k^{\dagger}\boldsymbol{D}_k\boldsymbol{\Theta}_k\boldsymbol{\Theta}_k^{\dagger}\boldsymbol{D}_k\boldsymbol{\Phi}_k + \boldsymbol{\Phi}_k^{\dagger}\boldsymbol{\Phi}_k, \tag{36}$$

$$\boldsymbol{\Phi}_k^{\dagger}\boldsymbol{D}_k\boldsymbol{\Theta}_k\boldsymbol{W}_k = \boldsymbol{\Theta}_k^{\dagger}\boldsymbol{D}_k\boldsymbol{\Phi}_k\boldsymbol{W}_k\boldsymbol{\Phi}_k^{\dagger}\boldsymbol{D}_k\boldsymbol{\Theta}_k + \boldsymbol{\Theta}_k^{\dagger}\boldsymbol{\Theta}_k. \tag{37}$$

From (36), we see that $\boldsymbol{\Phi}_k^{\dagger}\boldsymbol{D}_k\boldsymbol{\Theta}_k$ is Hermitian since the other terms are Hermitian. Similarly, $\boldsymbol{\Phi}_k^{\dagger}\boldsymbol{D}_k\boldsymbol{\Theta}_k\boldsymbol{W}_k$ in (37) is Hermitian since the other terms are Hermitian. Assuming that $\boldsymbol{W}_k$ has distinct diagonal entries, then $\boldsymbol{\Theta}_k$ and $\boldsymbol{\Phi}_k$ are diagonal since $\boldsymbol{\Phi}_k^{\dagger}\boldsymbol{D}_k\boldsymbol{\Theta}_k$ is Hermitian, $\boldsymbol{W}_k$ is diagonal, and their multiplication $\boldsymbol{\Phi}_k^{\dagger}\boldsymbol{D}_k\boldsymbol{\Theta}_k\boldsymbol{W}_k$ is Hermitian. For the case where the diagonal elements of $\boldsymbol{W}_k$ have repeated entries, we follow [17, 18] and add a perturbation matrix $\triangle_{\boldsymbol{W}_k}$ that ensures that the elements of $\boldsymbol{W}_k$ are distinct. Since $\boldsymbol{U}_k$ and

$\boldsymbol{V}_k$ are continuous functions of $\boldsymbol{W}_k$ in (28) and (29), and $\lim_{\triangle_{\boldsymbol{W}_k}\to\mathbf{0}} \boldsymbol{V}_k(\boldsymbol{W}_k + \triangle_{\boldsymbol{W}_k}) = \boldsymbol{V}_k(\boldsymbol{W}_k)$, then we can treat $\boldsymbol{\Phi}_k^\dagger \boldsymbol{D}_k \boldsymbol{\Theta}_k$ to be diagonal for any $\boldsymbol{W}_k$.

Now, we show that $\boldsymbol{\Phi}_k$ and $\boldsymbol{\Theta}_k$ have nonnegative diagonal entries. Let $\boldsymbol{\mathcal{D}}_1, \boldsymbol{\mathcal{D}}_2, \ldots$ denote diagonal matrices. Then, let

$$\boldsymbol{\mathcal{D}}_1 = \boldsymbol{\Phi}_k^\dagger \boldsymbol{D}_k \boldsymbol{\Theta}_k, \tag{38}$$

$$\boldsymbol{\mathcal{D}}_2 = \boldsymbol{\Phi}_k^\dagger \boldsymbol{\Phi}_k \succeq 0, \tag{39}$$

$$\boldsymbol{\mathcal{D}}_3 = \boldsymbol{\Theta}_k^\dagger \boldsymbol{\Theta}_k \succeq 0, \tag{40}$$

where $(\cdot) \succeq 0$ denotes that $(\cdot)$ is a positive semidefinite matrix. Let $\boldsymbol{\mathcal{U}}$ and $\boldsymbol{\mathcal{V}}$ be unitary matrices, then (39) and (40) can be rewritten as

$$\boldsymbol{\Phi}_k = \boldsymbol{\mathcal{U}} \boldsymbol{\mathcal{D}}_2^{1/2}, \tag{41}$$

$$\boldsymbol{\Theta}_k = \boldsymbol{\mathcal{V}} \boldsymbol{\mathcal{D}}_3^{1/2}. \tag{42}$$

Plugging in (41) and (42) into (38), we get

$$\begin{aligned} \boldsymbol{\mathcal{D}}_1 &= \boldsymbol{\mathcal{D}}_2^{1/2} \boldsymbol{\mathcal{U}}^\dagger \boldsymbol{D}_k \boldsymbol{\mathcal{V}} \boldsymbol{\mathcal{D}}_3^{1/2}, \\ \boldsymbol{\mathcal{D}}_4 &= \boldsymbol{\mathcal{D}}_2^{-1/2} \boldsymbol{\mathcal{D}}_1 \boldsymbol{\mathcal{D}}_3^{-1/2} = \boldsymbol{\mathcal{U}}^\dagger \boldsymbol{D}_k \boldsymbol{\mathcal{V}}. \end{aligned} \tag{43}$$

By left and right multiplication of (43) with its conjugate transpose, we get

$$\boldsymbol{\mathcal{D}}_4^2 = \boldsymbol{\mathcal{V}}^\dagger \boldsymbol{D}_k^2 \boldsymbol{\mathcal{V}}, \tag{44}$$

$$\boldsymbol{\mathcal{D}}_4^2 = \boldsymbol{\mathcal{U}}^\dagger \boldsymbol{D}_k^2 \boldsymbol{\mathcal{U}}, \tag{45}$$

respectively. From (44) and (45) , it is clear that

$$\boldsymbol{\mathcal{V}} = \boldsymbol{\mathcal{U}} = \boldsymbol{\mathcal{D}}_5, \tag{46}$$

where $\boldsymbol{\mathcal{D}}_5$ has elements $e^{j\theta_1}, \ldots, e^{j\theta_{d_k}}$ in its diagonal, for arbitrary $\theta_i \in [0, 2\pi]$. Because the choice of θ_i does not impose any restrictions on the solution, we choose $\theta_i = 0$ for all $i \in \{1, \ldots, d_k\}$ so that $\boldsymbol{\mathcal{D}}_5 = \boldsymbol{I}$. Therefore,

$$\boldsymbol{\Phi}_k = \boldsymbol{\mathcal{D}}_2^{1/2} \succeq 0, \tag{47}$$

$$\boldsymbol{\Theta}_k = \boldsymbol{\mathcal{D}}_3^{1/2} \succeq 0, \tag{48}$$

which proves that $\boldsymbol{\Phi}_k$ and $\boldsymbol{\Theta}_k$ are diagonal matrices with real nonnegative entries.

Finally, we derive (12) and (13). Simplifying (36) and (37) using (38), and then plugging in (47) and (48) into the resulting expressions and into (38), we get

$$\boldsymbol{\mathcal{D}}_1 = \boldsymbol{\mathcal{D}}_1^2 + \boldsymbol{\mathcal{D}}_2, \tag{49}$$

$$\boldsymbol{\mathcal{D}}_1 \boldsymbol{W}_k = \boldsymbol{\mathcal{D}}_1 \boldsymbol{W}_k \boldsymbol{\mathcal{D}}_1 + \boldsymbol{\mathcal{D}}_3, \tag{50}$$

$$\boldsymbol{\mathcal{D}}_1 = \boldsymbol{\mathcal{D}}_2^{1/2} \boldsymbol{D}_k \boldsymbol{\mathcal{D}}_3^{1/2}. \tag{51}$$

Solving (49) for $\boldsymbol{\mathcal{D}}_2$, (50) for $\boldsymbol{\mathcal{D}}_3$, plugging the results into (51), and simplifying, we get

$$\boldsymbol{W}_k^{1/2} \boldsymbol{\mathcal{D}}_1 \left(\boldsymbol{I} - \boldsymbol{\mathcal{D}}_1\right) \boldsymbol{D}_k = \boldsymbol{\mathcal{D}}_1. \tag{52}$$

Solving for $\boldsymbol{\mathcal{D}}_1$, we get

$$\boldsymbol{\mathcal{D}}_1 = \left(\boldsymbol{I} - \boldsymbol{W}_k^{-1/2} \boldsymbol{D}_k^{-1}\right)_+, \tag{53}$$

where $(\cdot)_+$ is necessary since $\boldsymbol{\mathcal{D}}_1 \succeq 0$. Plugging in (53) into (49) and (50) we get

$$\boldsymbol{\mathcal{D}}_2 = \left(\boldsymbol{W}_k^{-1/2} \boldsymbol{D}_k^{-1} - \boldsymbol{W}_k^{-1} \boldsymbol{D}_k^{-2}\right)_+, \tag{54}$$

$$\boldsymbol{\mathcal{D}}_3 = \left(\boldsymbol{W}_k^{1/2} \boldsymbol{D}_k^{-1} - \boldsymbol{D}_k^{-2}\right)_+. \tag{55}$$

Finally, plugging in (54) and (55) into (47) and (48), we get (13) and (12), respectively. □

References

[1] A. Molisch, *Wireless Communications*. Wiley-IEEE Press, 2005.

[2] K. Gomadam, V. Cadambe, and S. Jafar, "Approaching the capacity of wireless networks through distributed interference alignment," in *Proc. IEEE Globecom*, Dec. 2008, pp. 1–6.

[3] ——, "A distributed numerical approach to interference alignment and applications to wireless interference networks," *IEEE Trans. Inf. Theory*, vol. 57, no. 6, pp. 3309–3322, Jun. 2011.

[4] L. Cortés-Peña, J. Barry, and D. Blough, "The performance loss of unilateral interference cancellation," in *Proc. IEEE ICC*, Jun. 2012, pp. 4181–4186.

[5] F. Negro, S. Shenoy, I. Ghauri, and D. Slock, "On the MIMO interference channel," in *Inf. Theory Appl. Workshop*, Feb. 2010, pp. 1–9.

[6] S. Ye and R. Blum, "Optimized signaling for MIMO interference systems with feedback," *IEEE Trans. Signal Process.*, vol. 51, no. 11, pp. 2839–2848, Nov. 2003.

[7] G. Arslan, M. Demirkol, and Y. Song, "Equilibrium efficiency improvement in MIMO interference systems: A decentralized stream control approach," *IEEE Trans. Wireless Commun.*, vol. 6, no. 8, pp. 2984–2993, Aug. 2007.

[8] B. Hamdaoui and K. Shin, "Characterization and analysis of multi-hop wireless MIMO network throughput," in *ACM MobiHoc*, Sep. 2007, pp. 120–129.

[9] J. Liu, Y. Shi, and Y. Hou, "A tractable and accurate cross-layer model for multi-hop MIMO networks," in *Proc. IEEE Infocom*, Mar. 2010, pp. 1–9.

[10] Y. Shi, J. Liu, C. Jiang, C. Gao, and Y. Hou, "An optimal link layer model for multi-hop MIMO networks," in *Proc. IEEE Infocom*, Apr. 2011, pp. 1916–1924.

[11] R. Srinivasan, D. Blough, L. Cortés-Peña, and P. Santi, "Maximizing throughput in MIMO networks with variable rate streams," in *European Wireless Conf.*, Apr. 2010, pp. 551–559.

[12] D. Blough, G. Resta, P. Santi, R. Shrinivasan, and L. Cortés-Peña, "Optimal one-shot scheduling for MIMO networks," in *Proc. IEEE Secon*, Jun. 2011, pp. 404–412.

[13] R. Bhatia and L. Li, "Throughput optimization of wireless mesh networks with MIMO links," in *Proc. IEEE Infocom*, May 2007, pp. 2326–2330.

[14] S. Chu and X. Wang, "Opportunistic and cooperative spatial multiplexing in MIMO ad hoc networks," *IEEE/ACM Trans. Netw.*, vol. 18, no. 5, pp. 1610–1623, Oct. 2010.

[15] S. Peters and R. Heath, "Cooperative algorithms for MIMO interference channels," *IEEE Trans. Veh. Technol.*, vol. 60, no. 1, pp. 206–218, Jan. 2011.

[16] M. Razaviyayn, M. Sanjabi, and Z. Luo, "Linear transceiver design for interference alignment: Complexity and computation," *IEEE Trans. Inf. Theory*, vol. 58, no. 5, May 2012.

[17] H. Sampath, P. Stoica, and A. Paulraj, "Generalized linear precoder and decoder design for MIMO channels using the weighted MMSE criterion," *IEEE Trans. Commun.*, vol. 49, no. 12, pp. 2198–2206, Dec. 2001.

[18] S. Christensen, R. Agarwal, E. Carvalho, and J. Cioffi, "Weighted sum-rate maximization using weighted MMSE for MIMO-BC beamforming design," *IEEE Trans. Wireless Commun.*, vol. 7, no. 12, pp. 4792–4799, Dec. 2008.

[19] R. Blum, "MIMO capacity with interference," *IEEE J. Sel. Areas Commun.*, vol. 21, no. 5, pp. 793–801, Jun. 2003.

[20] F. Rashid-Farrokhi, K. Liu, and L. Tassiulas, "Transmit beamforming and power control for cellular wireless systems," *IEEE J. Sel. Areas Commun.*, vol. 16, no. 8, pp. 1437–1450, Oct. 1998.

[21] G. Foschini and M. Gans, "On limits of wireless communications in a fading environment when using multiple antennas," *Wireless Personal Commun.*, vol. 6, no. 3, pp. 311–335, Mar. 1998.